

SUPPLEMENTARY MATERIAL

Pathways and Mechanisms for Product Release in the Engineered Haloalkane Dehalogenases Explored Using Classical and Random Acceleration Molecular Dynamics Simulations

Martin Klvana¹, Martina Pavlova¹, Tana Koudelakova¹, Radka Chaloupkova¹, Pavel Dvorak¹, Zbynek Prokop¹, Alena Stsiapanava², Michal Kutý^{2,3}, Ivana Kuta-Smatanova^{2,3}, Jan Dohnalek⁴, Petr Kulhanek⁵, Rebecca C. Wade⁶ and Jiri Damborsky^{1,*}

¹Loschmidt Laboratories, Institute of Experimental Biology and National Centre for Biomolecular Research, Faculty of Science, Masaryk University, Kamenice 5/A4, 625 00 Brno, Czech Republic ²Institute of Physical Biology, University of South Bohemia České Budějovice, Zámek 136, 373 33 Nové Hradky, Czech Republic ³Institute of Systems Biology and Ecology, Academy of Sciences of the Czech Republic, Zámek 136, 373 33 Nové Hradky, Czech Republic ⁴Institute of Macromolecular Chemistry, Academy of Sciences of the Czech Republic, Heyrovského náměstí 2, 162 06 Praha 6, Czech Republic ⁵Laboratory of Computational Chemistry, National Centre for Biomolecular Research, Faculty of Science, Masaryk University, Kamenice 5/A4, 625 00 Brno, Czech Republic ⁶Molecular and Cellular Modeling Group, EML Research, Schloss-Wolfsbrunnenweg 33, D-69118 Heidelberg, Germany

*To whom correspondence may be addressed: Jiří Damborský, Loschmidt Laboratories, Institute of Experimental Biology and National Centre for Biomolecular Research, Faculty of Science, Masaryk University, Kamenice 5/A4, 625 00 Brno, Czech Republic, telephone: +420-549493467, fax: +420-549492556, jiri@chemi.muni.cz

Supplementary Figures:

Figure S1. Inhibition of TCP conversion by DCL product.

Figure S2. Far-UV CD spectra of wild-type DhaA and its mutants.

Figure S3. Docked conformations of DCL in wild-type DhaA complexed with CL.

Figure S4. Release of CL through p1 in the wild-type DhaA.

Figure S5. Release of CL through p1 in the 15 mutant.

Figure S6. Release of DCL through p1 in wild-type DhaA.

Figure S7. Release of DCL through p1 in the 04 mutant.

Figure S8. Release of DCL through p1 in the 31 mutant.

Figure S9. Release of DCL through p1 in the 51 mutant.

Figure S10. Release of DCL through p1 in the 52 mutant.

Figure S11. Release of DCL through p2a in wild-type DhaA.

Figure S12. Release of DCL through p2b in the 27 mutant.

Figure S13. Release of DCL through p2c in the 21 mutant.

Figure S14. Release of DCL through p3 in wild-type DhaA.

Figure S15. Selected attractive electrostatic and van der Waals interactions between DCL and protein residues during release of DCL through the different pathways.

Supplementary Tables:

Table S1. Overview of MD trajectories of wild-type DhaA and its mutants complexed with CL and DCL.

Table S2. Overview of MD trajectories of wild-type DhaA and its mutants complexed with DCL.

Table S3. Overview of RAMD trajectories of wild-type DhaA complexed with DCL.

Table S4. Overview of RAMD trajectories of DhaA mutants complexed with DCL.

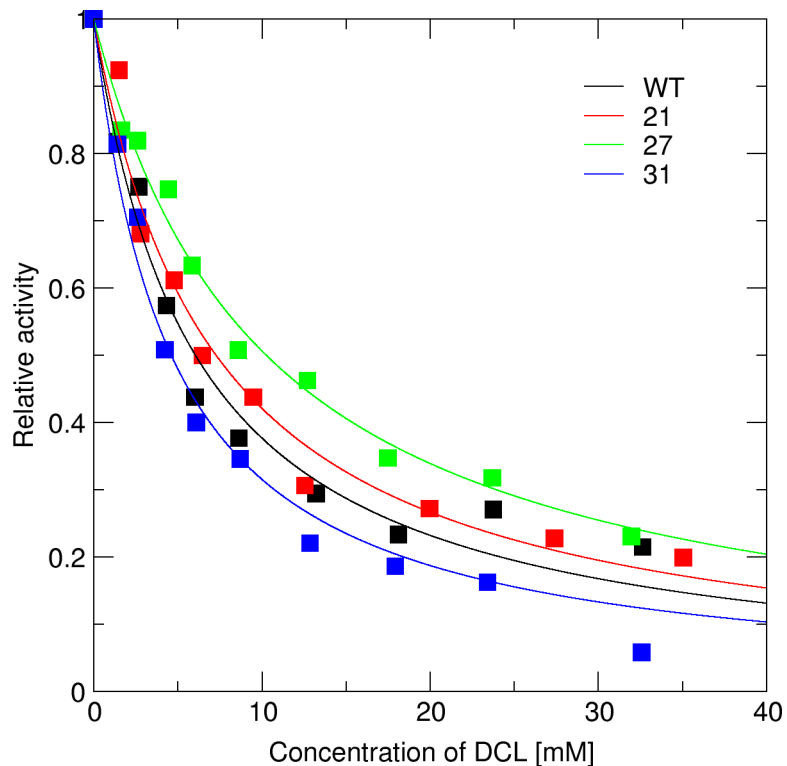


Figure S1. Inhibition of TCP conversion by DCL product. Data were fitted to the model for competitive inhibition expressed as $a = (K_m + [S]) / (K_m(1 + [I]/K_i) + [S])$, where a – relative activity, $[S]$ – concentration of TCP, and $[I]$ – concentration of DCL. $K_i^{wt} = 2.50 \pm 0.17$ mM, $K_i^{21} = 3.15 \pm 0.20$ mM, $K_i^{27} = 4.42 \pm 0.19$ mM, $K_i^{31} = 2.08 \pm 0.15$ mM.

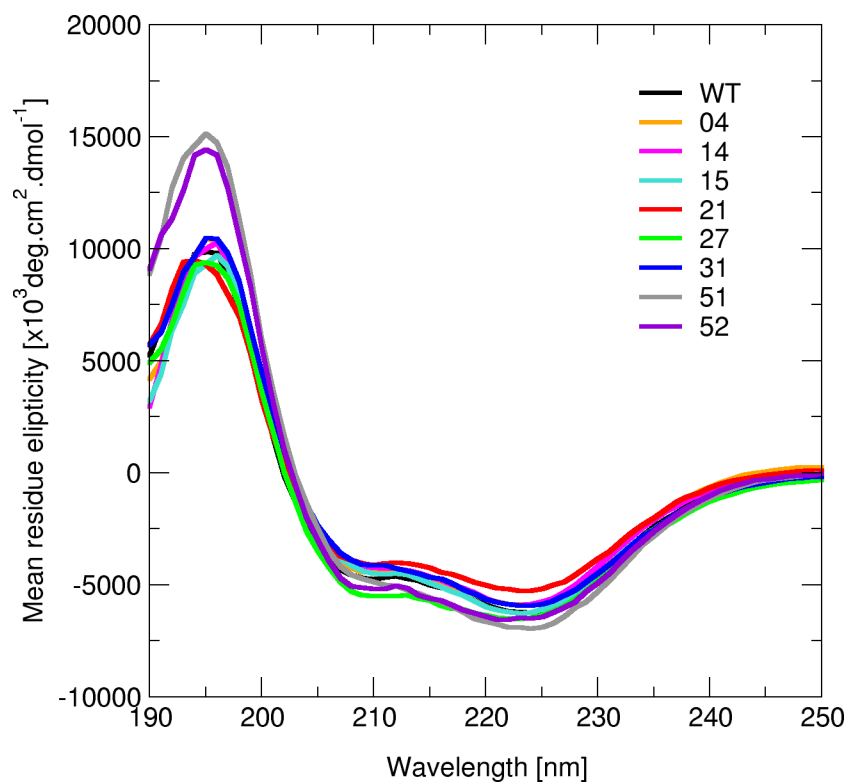


Figure S2. Far-UV CD spectra of wild-type DhaA and its mutants. The most similar spectra to the wild-type DhaA were determined with the 04, 14, 15, and 31. Compared to the wild-type DhaA, the 21 mutant shows higher mean residue ellipticity at 208 and 222 nm, while the mutants 27, 51 and 52 show lower mean residue ellipticity at 208 and 222 nm. The CD spectra of the wild-type DhaA and the 21, 27 and 31 mutants were adopted from Pavlova *et al.*¹

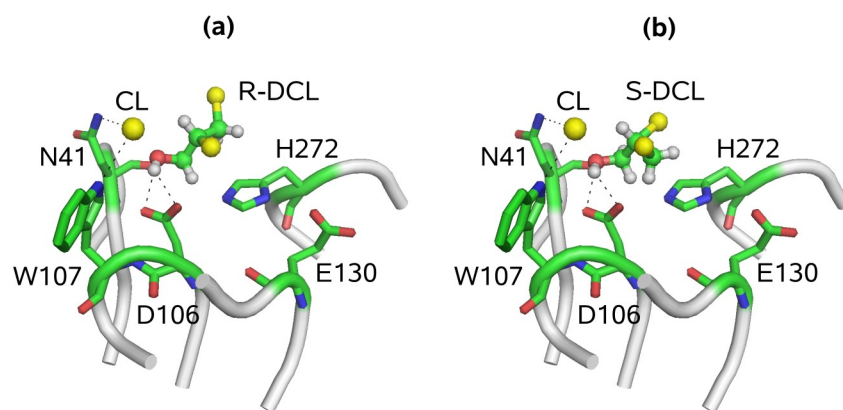


Figure S3. Docked conformations of DCL in wild-type DhaA complexed with CL. (*R*)-DCL (**a**), (*S*)-DCL (**b**). Catalytic pentad is in sticks, CL is represented by a sphere and DCL by balls and sticks. Dashed lines indicate hydrogen bonding interactions. All molecular graphics were created using PYMOL (DeLano Scientific, San Francisco, USA).

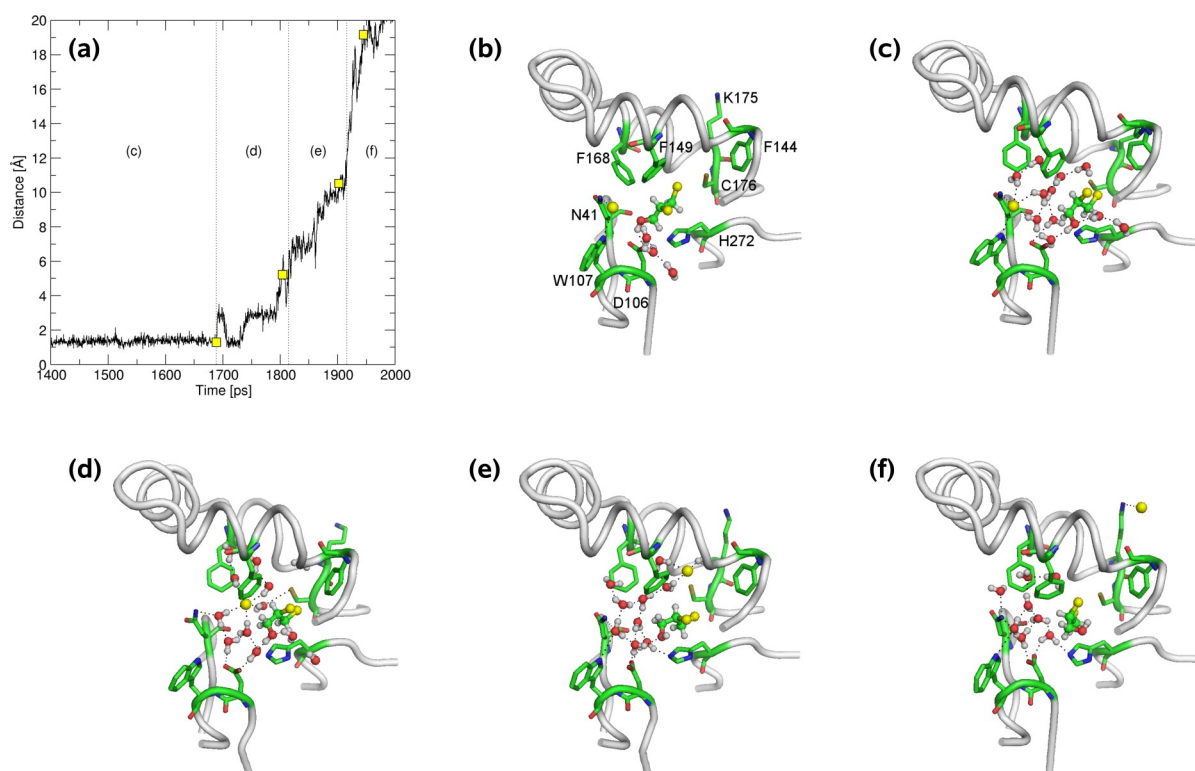


Figure S4. Release of CL through p1 in the wild-type DhaA. The graph shows distance of the CL from the halide stabilizing residues N41 and W107 (a). Representative snapshots are indicated by squares and depicted (b-f): the initial state (b), solvation of the active site (c), release of the CL from the halide-stabilizing residues (d), movement of the CL through p1 towards C176 (e) and release of the CL and water molecules to the bulk solvent with a transient interaction between the CL and K175 (f).

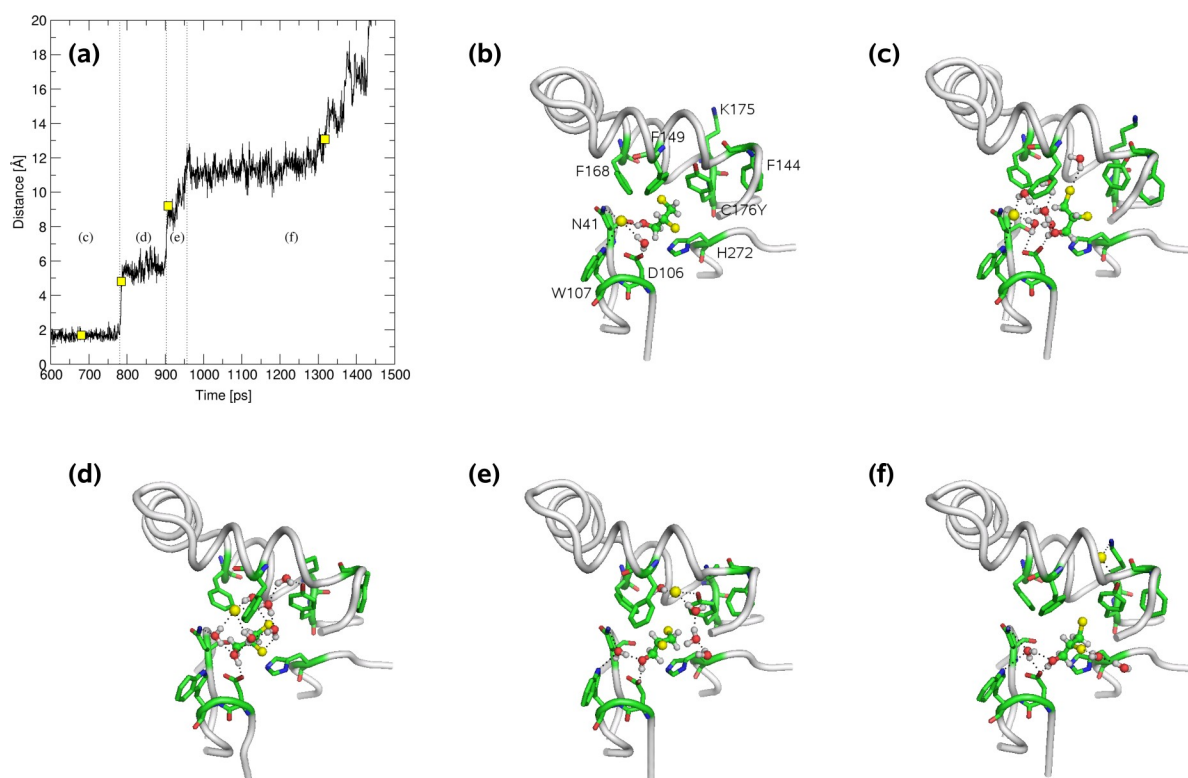


Figure S5. Release of CL through p1 in the 15 mutant. The graph shows distance of the CL from the halide stabilizing residues N41 and W107 (a). Representative snapshots are indicated by squares and depicted (b-f): the initial state (b), solvation of the active site (c), release of the CL from the halide-stabilizing residues (d), movement of the CL through p1 towards C176Y (e), and release of the CL and water molecules to the bulk solvent with transient interaction between the CL, C176Y and K175 (f).

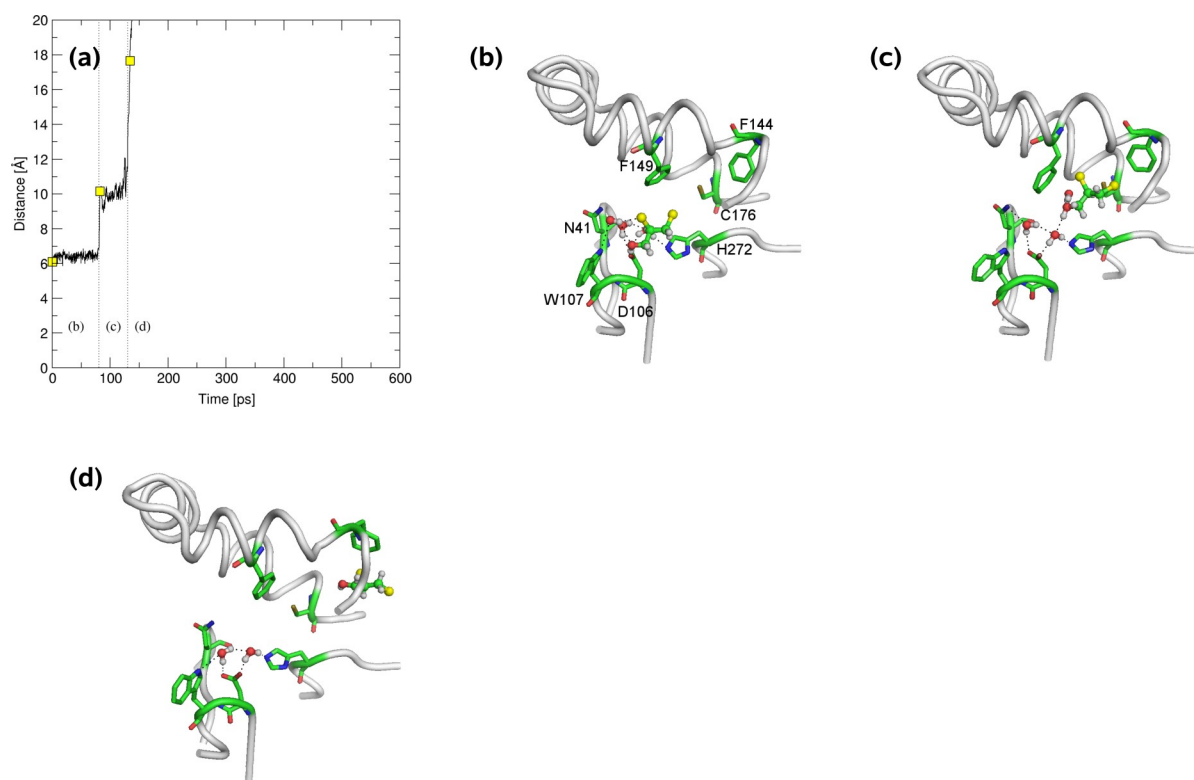


Figure S6. Release of DCL through p1 in wild-type DhaA. The graph shows distance of the DCL from the nucleophile D106 (a). Representative snapshots are indicated by squares and depicted (b-e): DCL-D106 hydrogen bonding interaction (b), DCL-water-D106 interaction (c), release of the DCL through p1 allowed by transient conformational change of F144 side chain (d).

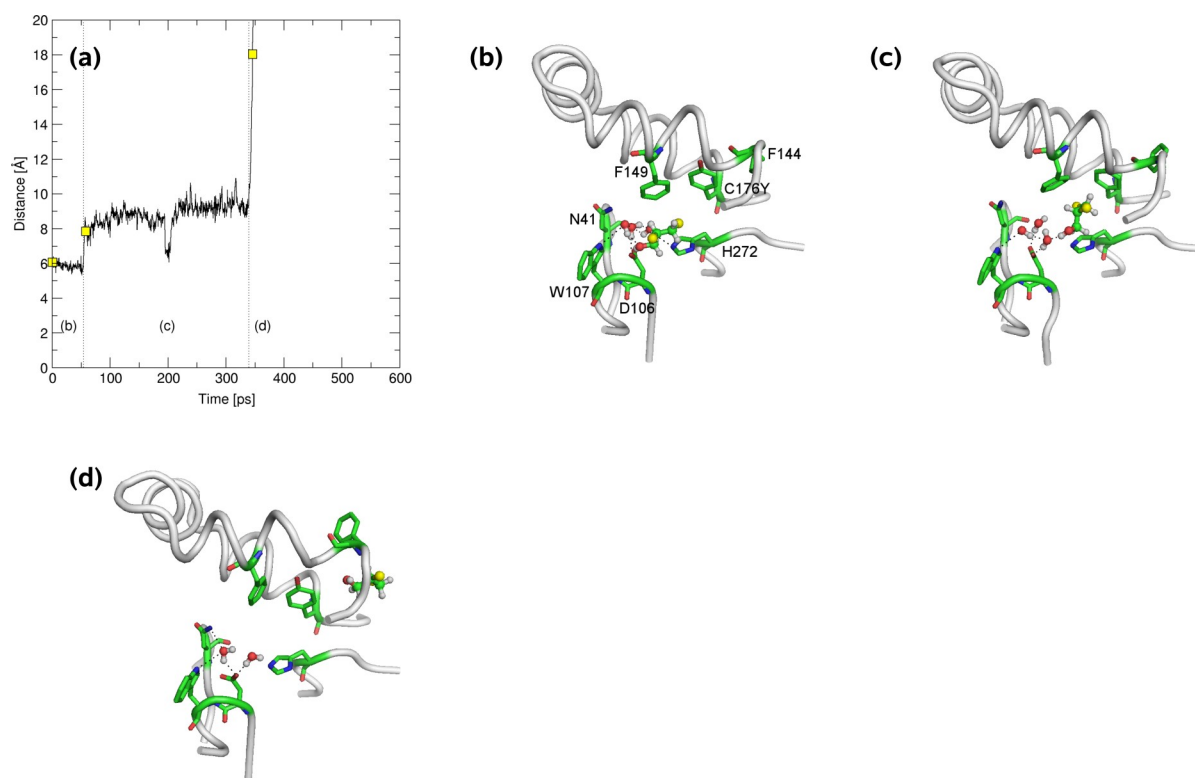


Figure S7. Release of DCL through p1 in the 04 mutant. The graph shows distance of the DCL from the nucleophile D106 **(a)**. Representative snapshots are indicated by squares and depicted **(b-e)**: DCL-D106 hydrogen bond **(b)**, DCL-water-D106 interaction **(c)**, release of the DCL through p1 allowed by transient conformational change of C176Y and F144 side chain **(d)**.

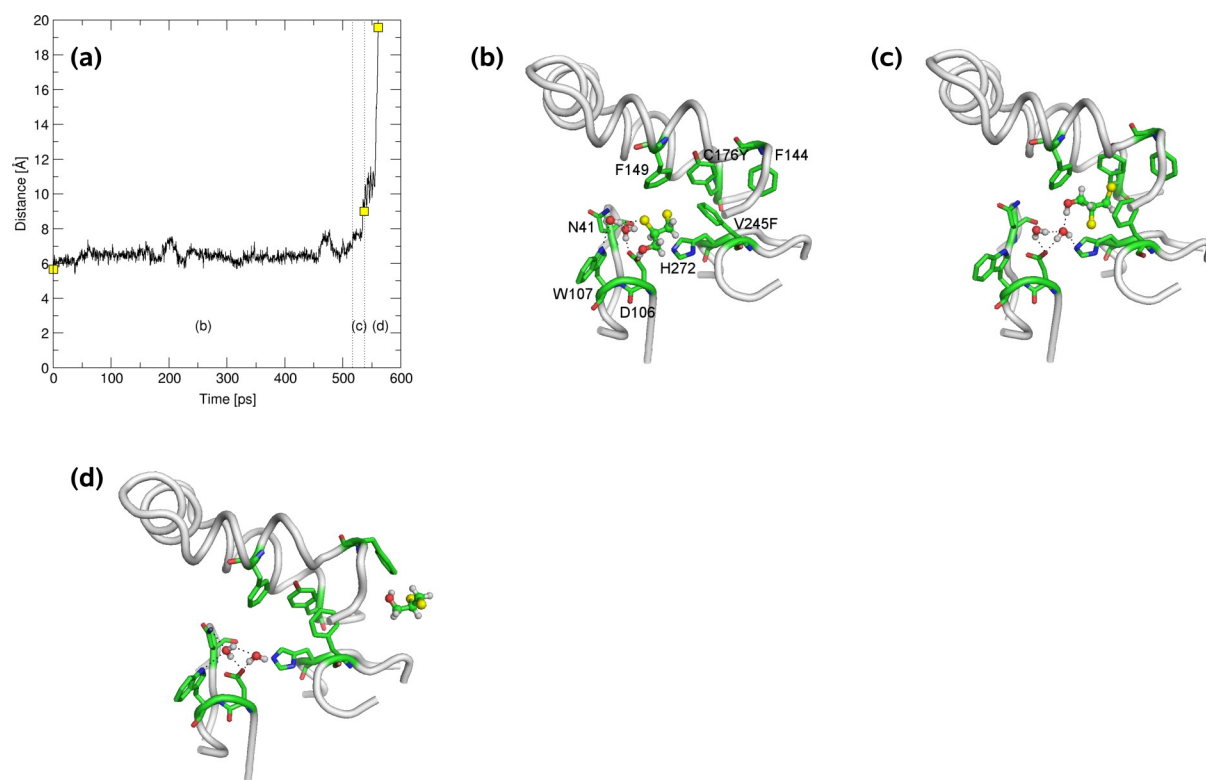


Figure S8. Release of DCL through p1 in the 31 mutant. The graph shows distance of the DCL from the nucleophile D106 (a). Representative snapshots are indicated by squares and depicted (b-d): DCL-D106 hydrogen bond (b), DCL-water-D106 interaction (c), release of the DCL through p1 allowed by transient conformational change of V245F and F144 side chain (d).

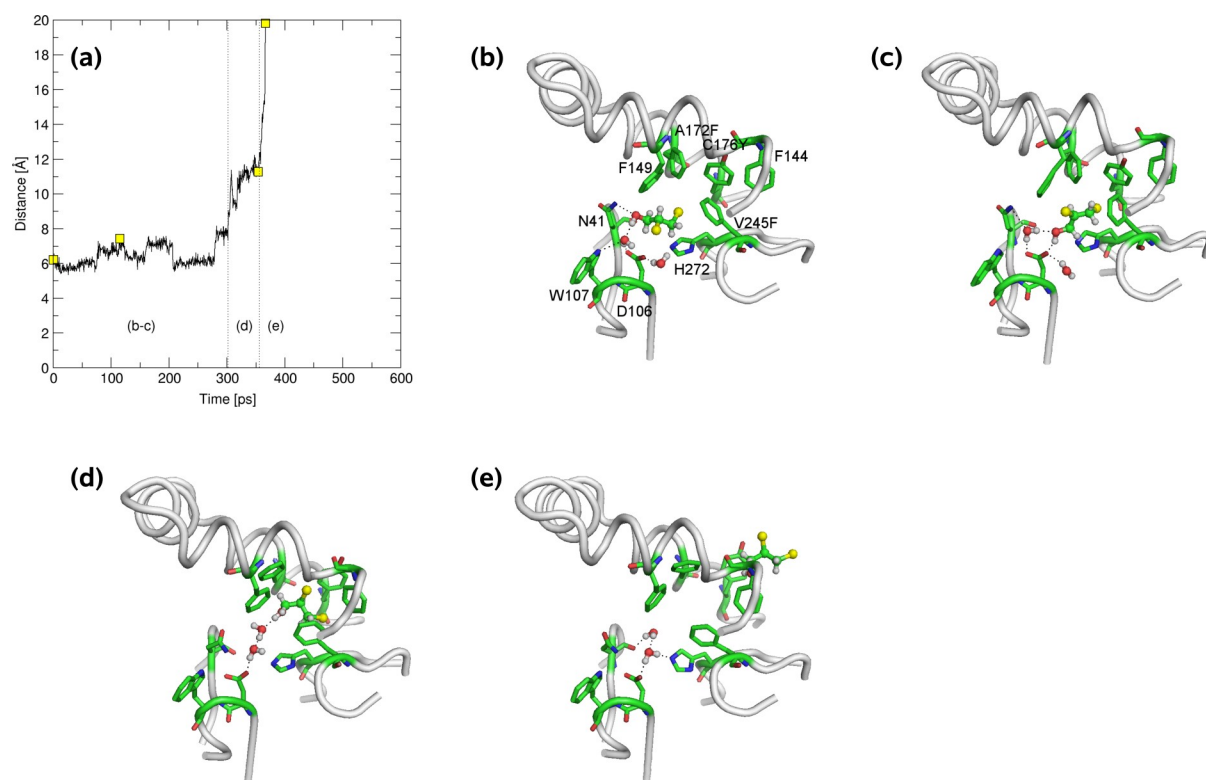


Figure S9. Release of DCL through p1 in the 51 mutant. The graph shows distance of the DCL from the nucleophile D106 (a). Representative snapshots are indicated by squares and depicted (b-e): DCL-D106 hydrogen bond (b), DCL-water-D106 interaction (c), movement of the DCL through p1 allowed by conformational change of A172F followed by conformational change of V245F and C176Y (d), release of the DCL to the bulk solvent allowed by transient conformational change of F144 side chain (e).

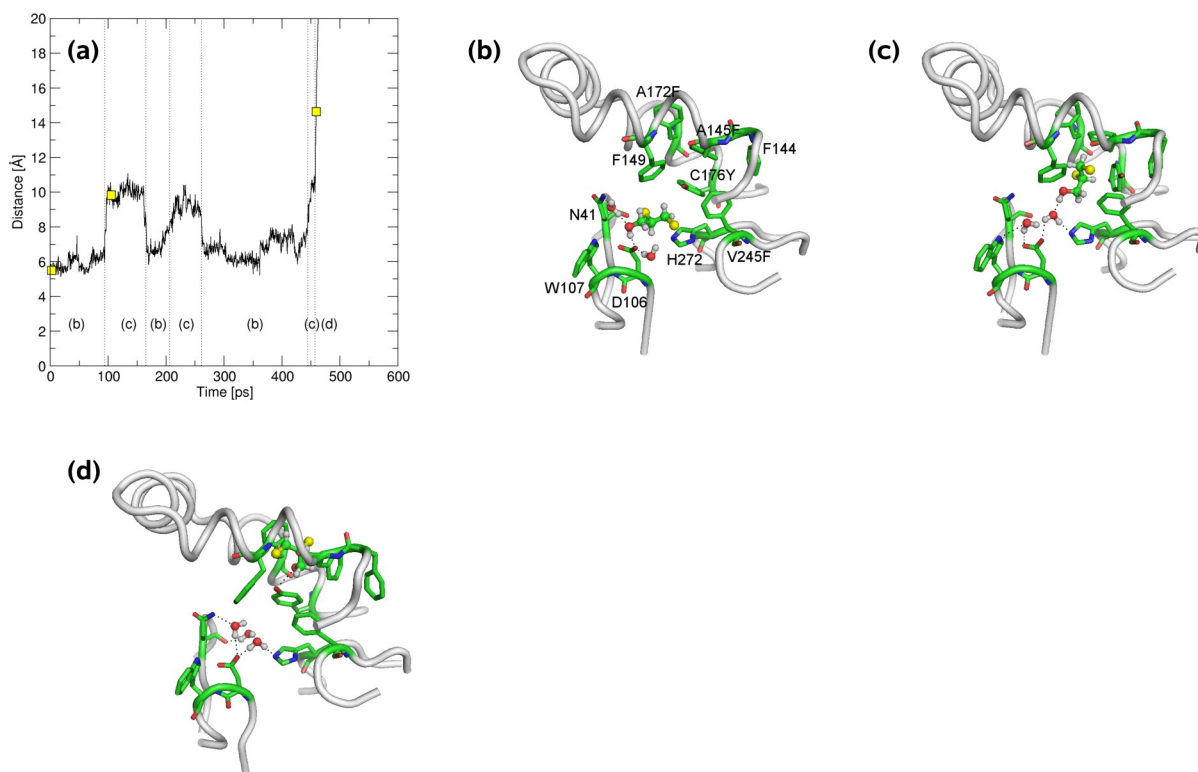


Figure S10. Release of DCL through p1 in the 52 mutant. The graph shows distance of the DCL from the nucleophile D106 (a). Representative snapshots are indicated by squares and depicted (b-d): DCL-D106 hydrogen bond (b), DCL-water-D106 interaction and consecutive conformational change of aromatic side chains of p1 (c), release of the DCL through p1 along A172F flipped to the bulk solvent due to interaction with A145F (d).

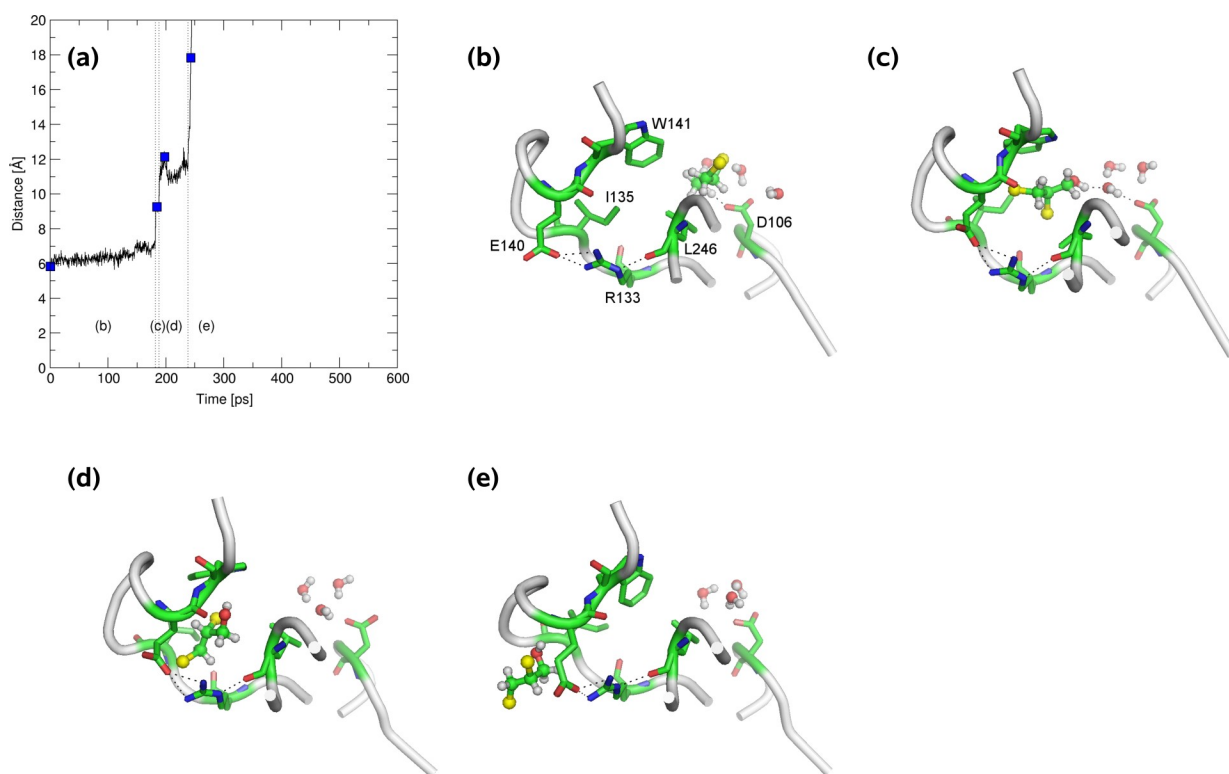


Figure S11. Release of DCL through p2a in wild-type DhaA. The graph shows distance of the DCL from the nucleophile D106 (a). Representative snapshots are indicated by squares and depicted (b-e): DCL-D106 hydrogen bond (b), DCL-water-D106 interaction (c), fast movement towards R133 (d), release of the DCL to the bulk solvent without perturbation of R133-E140 salt link (e).

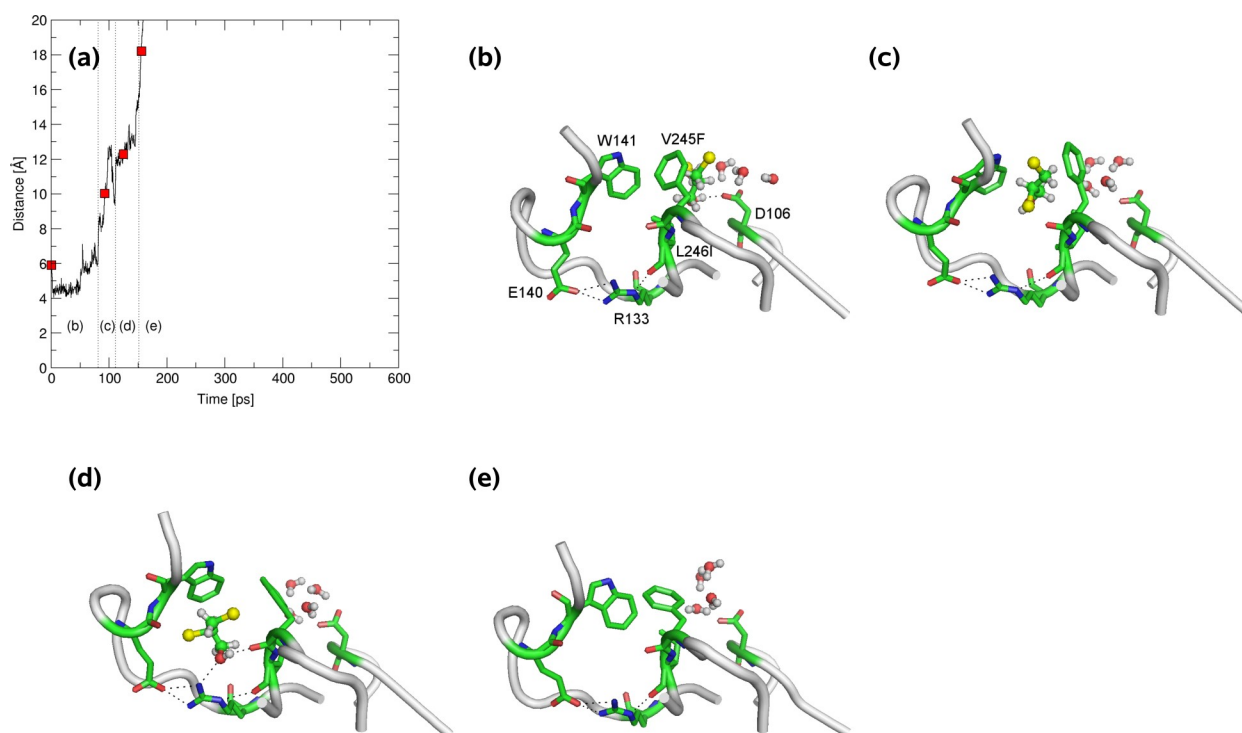


Figure S12. Release of DCL through p2b in the 27 mutant. The graph shows distance of the DCL from the nucleophile D106 (a). Representative snapshots are indicated by squares and depicted (b-e): DCL-D106 hydrogen bond (b), DCL-water-D106 interaction and progressive conformational change of W141 and V245F side chains (c), R133-DCL-V245F hydrogen bonds (d), release of the DCL to the bulk solvent and flip of W141 and V245F side chains to original conformation (e).

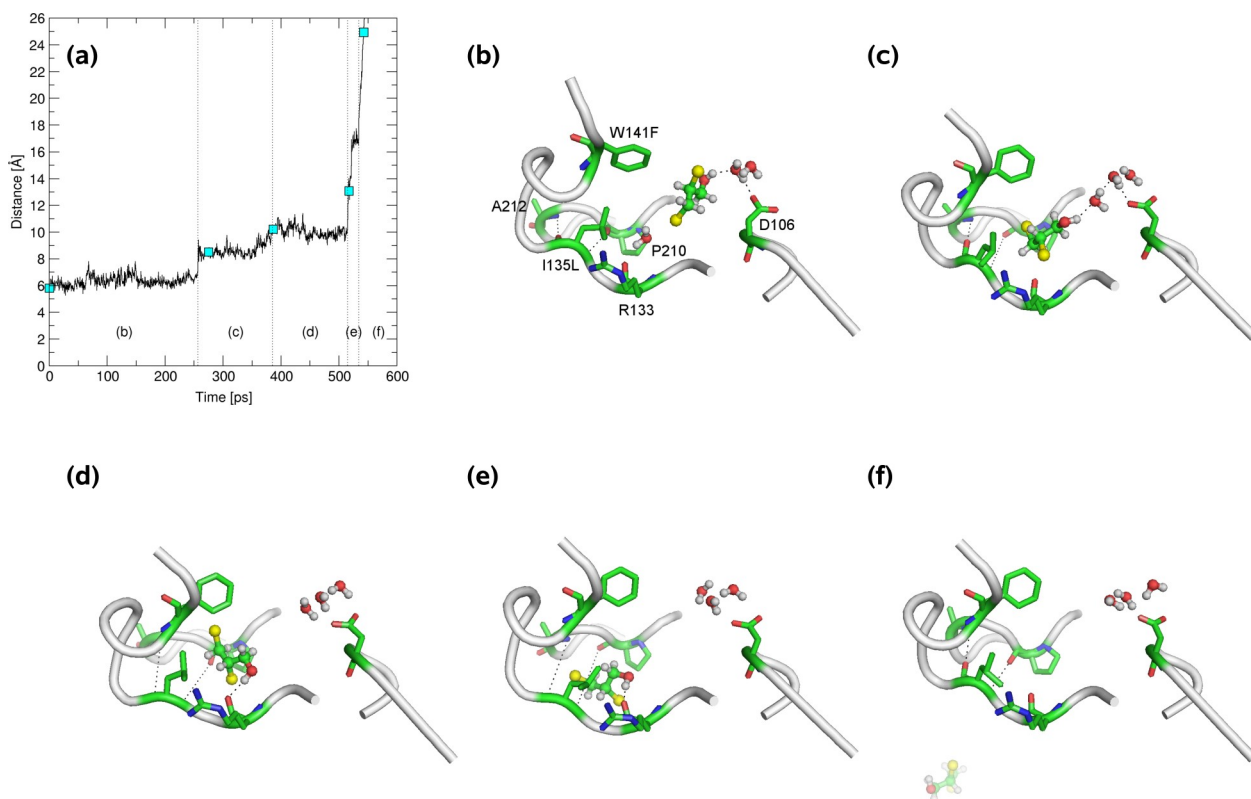


Figure S13. Release of DCL through p2c in the 21 mutant. The graph shows distance of the DCL from the nucleophile D106 (a). Representative snapshots are indicated by squares and depicted (b-e): DCL-D106 hydrogen bond (b), DCL-water-D106 interaction and perturbation of P210-I135L part of a β -bridge (c), DCL-R133 hydrogen bond and perturbation of A212-I135L part of the β -bridge (d), release of the DCL to the bulk solvent through the region of the original β -bridge (e), reconstruction of the β -bridge immediately after the release of the DCL (f).

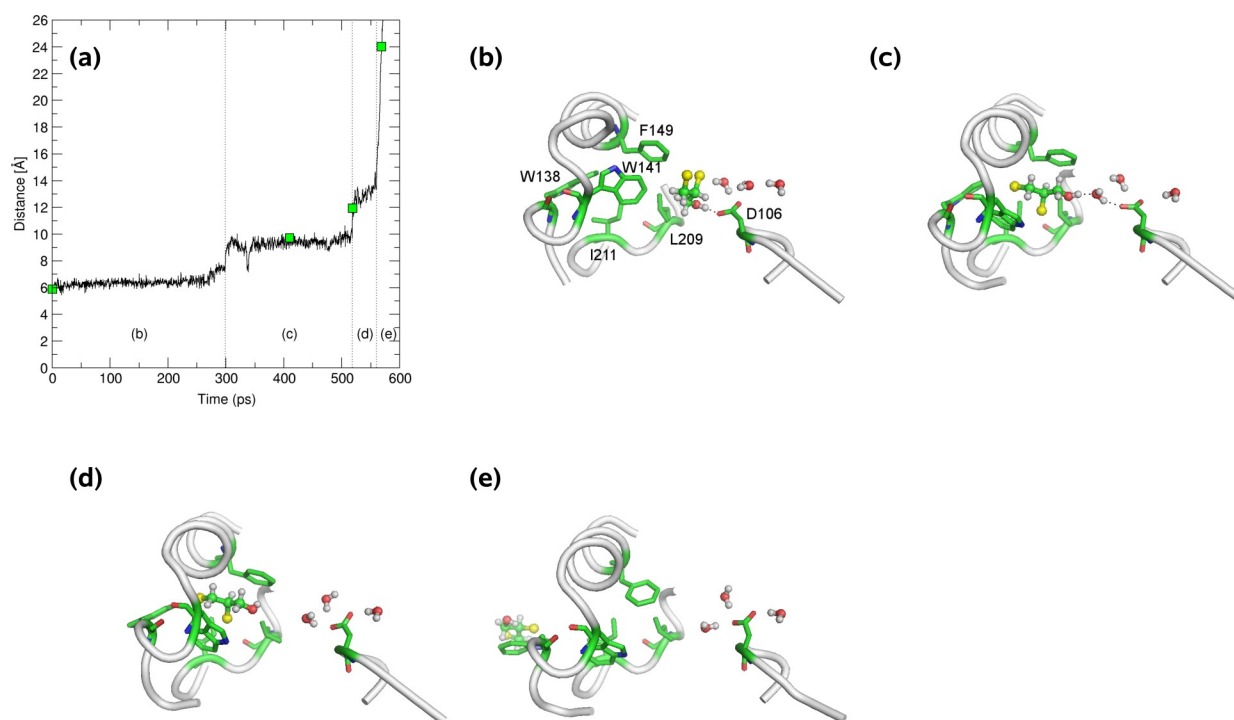


Figure S14. Release of DCL through p3 in wild-type DhaA. The graph shows distance of the DCL from the nucleophile D106 (a). Representative snapshots are indicated by squares and depicted (b-e): DCL-D106 hydrogen bond (b), DCL-water-D106 interaction and conformational change of W141 and F149 side chains (c), movement of DCL between W141 and F149 side chains, release of the DCL to the bulk solvent blocked by W138 (d), release of the DCL to the bulk solvent allowed by transient flip of W138 side chain to the bulk solvent (e).

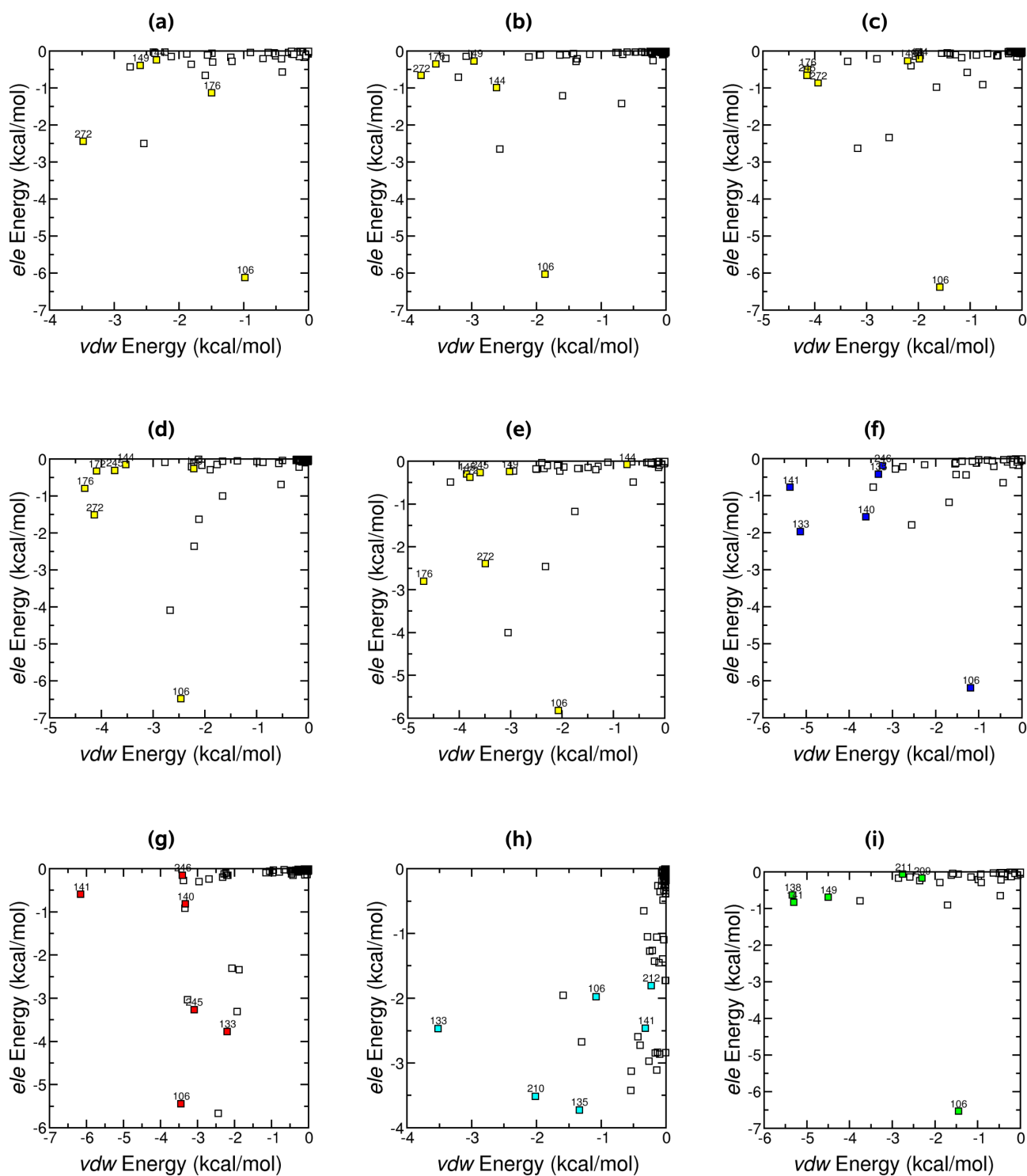


Figure S15. Selected attractive electrostatic (ele) and van der Waals (vdw) interactions between DCL and the protein residues during release of DCL through the different pathways: p1 in the wild-type DhaA (a), p1 in the 04 mutant (b), p1 in the 31 mutant (c), p1 in the 51 mutant (d), p1 in the 52 mutant (e), p2a in the wild-type DhaA (f), p2b in the 27 mutant (g), p2c in the 21 mutant (h), and p3 in the wild-type DhaA (i). The most important residues of the release pathways are annotated by residue identifier and color coded: p1 – yellow, p2a – blue, p2b – red, p2c – cyan, p3 – green.

Table S1. Overview of MD trajectories of wild-type DhaA and its mutants complexed with CL and DCL.

DhaA variant	Ligands	Length [ns]	Average RMSD of stable part [\AA] ^a	Timespan of stable RMSD [ns] ^b	Release pathway for DCL	Release pathway for CL
WT	<i>R</i> -DCL and CL	2.2	1.39 (± 0.03)	1.60 - 2.20	-	p1
	<i>S</i> -DCL and CL	2.8	1.55 (± 0.03)	1.85 - 2.80	-	-
04	<i>R</i> -DCL and CL	2.0	1.53 (± 0.03)	1.20 - 2.00	-	-
	<i>S</i> -DCL and CL	2.0	1.50 (± 0.02)	1.20 - 2.00	-	-
14	<i>R</i> -DCL and CL	2.0	1.33 (± 0.02)	1.25 - 2.00	-	-
	<i>S</i> -DCL and CL	2.0	1.43 (± 0.02)	1.30 - 2.00	-	-
15	<i>R</i> -DCL and CL	2.0	1.33 (± 0.02)	1.45 - 2.00	-	p1
	<i>S</i> -DCL and CL	2.0	1.37 (± 0.03)	1.45 - 2.00	-	-
21	<i>R</i> -DCL and CL	2.0	1.29 (± 0.04)	0.60 - 2.00	-	-
	<i>S</i> -DCL and CL	2.0	1.57 (± 0.04)	1.00 - 2.00	-	-
27	<i>R</i> -DCL and CL	2.0	1.43 (± 0.02)	1.70 - 2.00	-	-
	<i>S</i> -DCL and CL	2.0	1.41 (± 0.03)	1.30 - 2.00	-	-
31	<i>R</i> -DCL and CL	2.0	1.44 (± 0.02)	1.65 - 2.00	-	-
	<i>S</i> -DCL and CL	2.0	1.47 (± 0.03)	1.00 - 2.00	-	-
51	<i>R</i> -DCL and CL	2.0	1.43 (± 0.03)	0.90 - 2.00	-	-
	<i>S</i> -DCL and CL	2.0	1.42 (± 0.03)	1.40 - 2.00	-	-
52	<i>R</i> -DCL and CL	2.0	1.58 (± 0.02)	1.50 - 2.00	-	-
	<i>S</i> -DCL and CL	2.0	1.67 (± 0.03)	1.55 - 2.00	-	-

^aStandard deviation is given in parenthesis.

'-' No release.

Table S2. Overview of MD trajectories of wild-type DhaA and its mutants complexed with DCL.

DhaA variant	Ligand	Length [ns]	Average RMSD of stable part [\AA] ^a	Timespan of stable RMSD [ns] ^b	Release pathway for DCL
WT	R-DCL	2.8	1.38 (± 0.02)	1.85 - 2.80	-
	S-DCL	2.8	1.45 (± 0.02)	1.85 - 2.80	-
04	R-DCL	2.0	1.33 (± 0.03)	1.20 - 2.00	-
	S-DCL	2.0	1.34 (± 0.02)	1.20 - 2.00	-
14	R-DCL	2.0	1.36 (± 0.04)	0.90 - 2.00	-
	S-DCL	2.0	1.31 (± 0.03)	1.20 - 2.00	-
15	R-DCL	2.0	1.34 (± 0.02)	1.30 - 2.00	-
	S-DCL	2.0	1.29 (± 0.03)	1.30 - 2.00	-
21	R-DCL	2.0	1.29 (± 0.03)	0.80 - 2.00	-
	S-DCL	2.0	1.33 (± 0.05)	0.80 - 2.00	-
27	R-DCL	2.0	1.34 (± 0.02)	1.05 - 2.00	-
	S-DCL	2.0	1.31 (± 0.02)	1.25 - 2.00	-
31	R-DCL	2.0	1.35 (± 0.03)	1.15 - 2.00	-
	S-DCL	2.0	1.36 (± 0.03)	1.15 - 2.00	-
51	R-DCL	2.0	1.59 (± 0.01)	1.70 - 2.00	-
	S-DCL	2.0	1.43 (± 0.02)	1.35 - 2.00	-
52	R-DCL	2.0	1.37 (± 0.04)	0.80 - 2.00	-
	S-DCL	2.0	1.47 (± 0.03)	0.70 - 2.00	-

^aStandard deviation is given in parenthesis.

'-' No release.

Table S3. Overview of RAMD trajectories^a of wild-type DhaA complexed with DCL.

Ligand	Starting snapshot of MD [id]	Random acceleration [kcal Å ⁻¹ g ⁻¹]	RAMD threshold distance [Å]	Length [ps]	Release pathway for DCL
R-DCL	5178	0.04	0.002	1000	-
			0.004	480	p1
		0.05	0.002	102	p1
			0.004	60	p1
	5400	0.04	0.002	1000	-
			0.004	146	p1
		0.05	0.002	173	p2a
			0.004	143	p1
	5600	0.04	0.002	572	p3
			0.004	270	p1
		0.05	0.002	248	p2a
			0.004	99	p1
S-DCL	5194	0.04	0.002	157	p1
			0.004	43	p1
		0.05	0.002	185	p1
			0.004	35	p1
	5398	0.04	0.002	1000	-
			0.004	220	p1
		0.05	0.002	291	p1
			0.004	135	p1
5582	0.04	0.002	141	p1	
		0.004	305	p1	
	0.05	0.002	1000	-	
		0.004	160	p1	

^aNumber of steps = 10.

'-' No release.

Table S4. Overview of RAMD trajectories^{a,b} of DhaA mutants complexed with DCL.

DhaA variant	Ligand	Random acceleration [kcal Å ⁻¹ g ⁻¹]	RAMD threshold distance [Å]	Length [ps]	Release pathway for DCL
04	<i>R</i> -DCL	0.04	0.002	1000	-
			0.004	351	p1
		0.05	0.002	69	p1
			0.004	188	p1
	<i>S</i> -DCL	0.04	0.002	1000	-
			0.004	1000	-
		0.05	0.002	408	p2a
			0.004	106	p1
14	<i>R</i> -DCL	0.04	0.002	270	p1
			0.004	196	p1
		0.05	0.002	252	p1
			0.004	613	p1
	<i>S</i> -DCL	0.04	0.002	176	p1
			0.004	1000	-
		0.05	0.002	1000	-
			0.004	43	p1
15	<i>R</i> -DCL	0.04	0.002	1000	-
			0.004	183	p1
		0.05	0.002	1000	-
			0.004	85	p1
	<i>S</i> -DCL	0.04	0.002	1000	-
			0.004	1000	-
		0.05	0.004	588	p1
21	<i>R</i> -DCL	0.04	0.002	1000	-
			0.004	356	p1
		0.05	0.002	1000	-
			0.004	165	p1
	<i>S</i> -DCL	0.04	0.002	140	p1
			0.004	545	p2c
		0.05	0.002	1000	-
			0.004	232	p1

^aNumber of steps = 10.^bStarting snapshot = 4000.

'-' No release.

Table S4. (continued)

DhaA variant	Ligand	Random acceleration [kcal Å ⁻¹ g ⁻¹]	RAMD threshold distance [Å]	Length [ps]	Release pathway for DCL
27	<i>R</i> -DCL	0.04	0.002	230	p1
			0.004	200	p2b
		0.05	0.002	1000	-
			0.004	155	p3
	<i>S</i> -DCL	0.04	0.002	276	p1
			0.004	1000	-
0.002			1000	-	
31	<i>R</i> -DCL	0.04	0.002	1000	-
			0.004	565	p1
		0.05	0.002	1000	-
			0.004	1000	-
	<i>S</i> -DCL	0.04	0.002	1000	-
			0.004	1000	-
0.002			1000	-	
51	<i>R</i> -DCL	0.04	0.002	148	p1
			0.004	372	p1
		0.05	0.002	359	p1
			0.004	44	p1
	<i>S</i> -DCL	0.04	0.002	1000	-
			0.004	1000	-
0.002			1000	-	
52	<i>R</i> -DCL	0.04	0.002	1000	-
			0.004	465	p1
		0.05	0.002	239	p1
			0.004	28	p1
	<i>S</i> -DCL	0.04	0.002	1000	-
			0.004	1000	-
0.002			128	p1	
			0.004	273	p1

^aNumber of steps = 10.^bStarting snapshot = 4000.

'-' No release.

Supplementary References

1. Pavlova, M., Klvana, M., Prokop, Z., Chaloupkova, R., Banas, P., Otyepka, M., Wade, R.C., Nagata, Y., & Damborsky, J. (2009). Engineering access tunnels of dehalogenase by computational design and directed evolution to boost its activity towards an anthropogenic toxic substrate. *Nat. Chem. Biol.* (in press).